PHYSICAL REVIEW E **79**, 060402(R) (2009)

Diffusion through colloidal shells under stress

J. Guery,[1] J. Baudry,[1] D. A. Weitz,[2] P. M. Chaikin,[3] and J. Bibette[1]
[1]*Laboratoire Colloïdes et Matériaux divisés, ESPCI ParisTech, UPMC, CNRS UMR 7195, 10 rue Vauquelin, 75005 Paris, France*
[2]*Department of Physics, Harvard University, Cambridge, Massachusetts 02138, USA*
[3]*Department of Physics, New York University, New York, New York 10012, USA*
(Received 4 June 2008; published 29 June 2009)

The permeability of solids has long been associated with a diffusive process involving activated mechanism as originally envisioned by Eyring. Tensile stress can affect the activation energy but definitive experiments of the diffusion rate of species through a stressed solid are lacking. Here we use core-shell (liquid core–solid shell) colloidal particles that are sensitive to osmotic pressure to follow the permeation of encapsulated probes at various stresses. We unambiguously show that the tensile stress applied on colloidal shells linearly reduces the local energy barrier for diffusion.

DOI: 10.1103/PhysRevE.79.060402 PACS number(s): 82.70.Kj, 51.20.+d, 66.10.C−, 66.30.−h

Efficient storage of gases and liquids in solid containers is of tremendous technological and economical importance. This concerns almost all types of industrial domains, from the oil industry to food packaging [1], and the shell material may vary from metal to rubber to gel. At the same time, efficient encapsulation of active ingredients such as drugs, proteins, vitamins, flavors, or nutrients is essential for a myriad of applications, from drug delivery to food neutriceuticals and from cosmetics to agrichemicals [2,3]. The goal of such encapsulation is to protect delicate substances from a harsh environment and to retain their activity until required. Long-term storage of liquids or gases very often involves internal pressure, which increases the tensile stress of the container wall. At a colloidal scale hydrostatic pressure is not relevant; instead it is the osmotic pressure difference between the interior and the external medium that may similarly stress the shell of the colloidal scaffold. The Eyring model is often evoked to account for the effect of stress and deformation on the permeability of solids [4]. Aside from the technological consequences it is important to fundamentally understand these ideas and test them quantitatively. In Eyring's original paper [5] the forces and stresses act on the diffusing species, and the activation energy is directly reduced in a worklike manner, stress times volume. In the present case we consider diffusing probe particles permeating a solid shell, which is stressed by a force, which acts on the shell and not the probe. To investigate these conditions, we use core-shell (liquid core–solid shell) colloidal particles on which we can apply a controlled tensile stress by varying the external osmotic pressure. We then follow the average permeation of an encapsulated salt probe within a large colloidal population. Our results unambiguously demonstrate an activated mechanism and the phenomenological relationship that links stress and permeation. We find that the activation energy associated with the permeation process is decreased in proportion to the applied tensile stress even though the diffusing species are not submitted to any extra forces.

We create nearly monodisperse colloidal shells using a double emulsion consisting of droplets of water in larger drops of crystallizable oil. The oil is a mixture of crystallizable triglycerides, allowing us to formulate the emulsion at high temperature, 70 °C, where the oil is fluid, and then cool the sample to solidify the oil, creating a robust shell [6]. We use a triglyceride oil, DM [7], which is comprised of a broad distribution of triglycerides and forms an amorphous solid, as confirmed by differential scanning calorimetry (DSC), which reveals solidification over a broad distribution of temperatures (data not shown). The double emulsions are prepared in a two-step process [8]: we use a Couette device [9] to create an inverse water-in-oil emulsion, consisting of water droplets with a diameter of 400 nm and a polydispersity of ~25% [10]. The droplets are stabilized through addition of a sorbitan monoleate surfactant [11] in the oil and 0.4*M* NaCl in the water, which prevents ripening of the droplets. The final double emulsion is formed with a second emulsification step, using the inverse emulsion at a water-droplet volume fraction of ϕ_ι=0.4. We add 0.5 wt % alginate as a thickener to control the size [9] and obtain globules with a diameter d_g=4 μm, a polydispersity of less than 20% [10], and a globule volume fraction of ϕ_g=0.6. The globules are stabilized through addition of a surfactant to the continuous water phase; we use a diblock polyethylene glycol phospholipid at 8 wt % [11]. In addition, we add 0.65*M* glucose to match the chemical potential of the inner water to the continuous phase water. We deduce the osmotic pressure difference from the concentration of salt and glucose using tabulated values [15]. The final double emulsion is diluted to a volume fraction of ϕ_g=0.2 using a 0.65*M* glucose solution and is cooled to 0 °C to solidify the oil. The globule surface is at least partially crystalline, as evidenced by the faceted structure seen in the scanning electron microscopy (SEM) image, shown in Fig. 1(a). This yields a robust solid shell provided that the temperature is maintained below the melting temperature of the oil of about 45 °C. Nevertheless, globules can be broken during the harsh condition of SEM samples preparation, as shown in Fig. 1(b). For the broken globules we only see the outer shells and never the presence of interstitial walls separating inner droplets. We hypothesize that upon cooling, the latent heat of crystallization causes solidification to begin from the outside, creating a solid shell surrounding a liquid core comprised of any residual oil and the concentrated water droplets separated by very thin walls. The shell thickness can then be estimated from volume conservation to be about 100 nm.

We use potentiometric titration to measure the concentration of chloride ions as they are released into the continuous

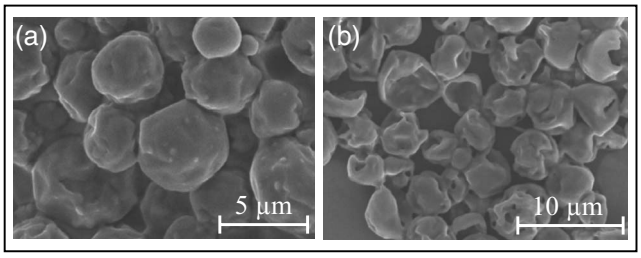

FIG. 1. Crystallizable double emulsions imaged with scanning electron microscope. (a) Typical image of globules. (b) With broken globules, only the outer shell is visible.

water phase [12]. We determine the relative ionic concentration in the water outside the colloids, X, by normalizing the concentration measured at each time by the value obtained when all ions are released. In Fig. 2(a), we show this fractional release X, as a function of time at different temperatures ranging from 15 to 65 °C for the DM oil. At 15 °C the oil is essentially solid, while at 65 °C it is entirely melted. Careful observation under a microscope shows no coalescence of the inner droplets with the globule interface in agreement with previous work [13]. Instead, the measured release must result entirely from the diffusion of sodium and chloride ions from inner droplets toward external phase. Such passive permeation must obey Fick's law given by $J=-dN_i/dt=PS(C_i-C_e)$, where J is the flux of salt from inside toward the external phase, N_i is the total number of salt ions inside the globule, P is the permeation coefficient of the shell, S is the total shell surface, and C is the concentration of salt inside (i) and in the external phase (e) [13]. We assume as in [13] that the limiting step is the permeation through the outer shell. The oil film between inner water droplets is much thinner than the shell thickness as seen in our SEM images. Hence the salt concentration C_i is essentially homogeneous within the inner water droplets during the leakage process. If the globule volume fraction ϕ is small, we have

$$dX/dt = \beta_0(1 - X), \tag{1}$$

where the ion concentration $X=C_e(t)/C_e(t=\text{infinity})$, and where $\beta_0=3P/a$ is the characteristic relaxation rate, with a being the globule radius. Therefore $X(t)=1-[(1-X_0)\exp(-\beta_0 t)]$, where X_0 is the initial burst fractional release which arises during the double emulsification process. For all temperatures studied the release mechanism is well described by a single exponential relaxation of time scale $1/\beta_0$, in agreement with the original Eyring assumption that the permeation coefficient P is proportional to $\exp(-E_a/k_BT)$ [5], where E_a is the activation energy and k_BT is the thermal energy. In Fig. 2(b), we plot $\ln \beta_0$ as a function of $1/k_BT$, from which we deduce the activation energy $E_a \sim (5-7)k_BT_r$, $T_r=25$ °C. In the absence of osmotic mismatch the leakage of our colloidal system is strictly diffusion driven, with no discontinuity at the liquid-solid transition again in agreement with the Eyring picture.

Dilution of the double emulsion by a factor of 100 using pure water leads to an osmotic pressure difference of $\Delta\Pi=17$ atm. Because there is a slight but sufficient permeability of water through the shell the chemical potential of the water equilibrates rapidly resulting in an immediate increase in the internal pressure. At 15 °C where the DM oil shell is solid, there is a rapid increase in the release of Cl^- ions followed by slower approach to the asymptotic limit, as shown by the open squares in Fig. 3(a). We vary the driving osmotic pressure, $\Delta\Pi$, by using water with increasing concentrations of glucose, diluting the double emulsion by the same factor each time; this reduces the rate of release. For $\Delta\Pi=0$, there is a residual very slow release of Cl^- shown by the open circles in Fig. 3(a). For $\Delta\Pi\neq 0$, the osmotic pressure mismatch causes a tensile stress on the shell, which should modify the activation energy. To check this hypothesis we must consider the relation between the osmotic pressure difference and the resulting tensile stress that acts on the colloidal shell. In the limit of a thin shell of thickness δ, this relation can be simply derived from a force balance argument. The force exerted by the osmotic pressure mismatch on each half shell, $\pi a^2\Delta\Pi$, and the force due to the tensile stress, τ, acting on the perimeter that holds the two half shells together, $2\pi a\delta\tau$, must be equal, $\tau=\Delta\Pi(a/2\delta)$ [14]. Part of the local activation energy E_a for an ion permeating a solid comes from the deformation energy of adding its additional volume to the solid matrix. The worklike energy for adding this volume increases under compressive stress and

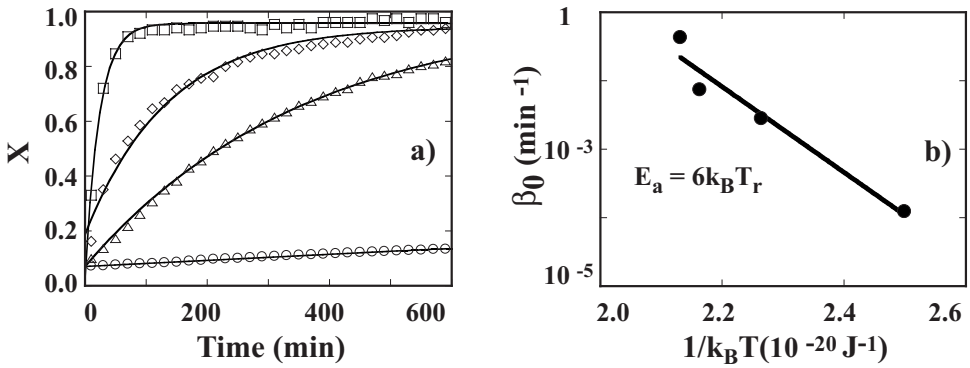

FIG. 2. (a) Temporal evolution of the fractional release (X) for a shell composed of pure oil DM, at different temperatures: (○) 15 °C; (△) 45 °C; (◇) 60 °C; and (□) 65 °C. The solid lines correspond to the best adjustment of the data with the equation: $X(t)=1-[(1-X_0)\exp(-\beta_0 t)]$. (b) Evolution of the characteristic relaxation rate (β_0) in logarithmic scale with $1/k_BT_r$. The solid line corresponds to an exponential adjustment.

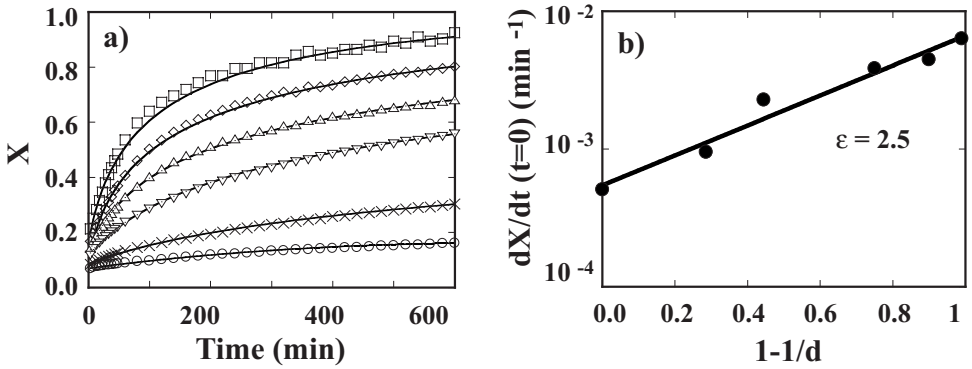

FIG. 3. (a) Temporal evolution of the fractional release (X), for different dilution factors ($T=15\,^{\circ}$C): (○) $d=0$, $\Delta\Pi=0$ atm; (×) $d=1.4$, $\Delta\Pi=5$ atm; (▽) $d=1.8$, $\Delta\Pi=8$ atm; (△) $d=4$, $\Delta\Pi=13$ atm; (◇) $d=10$, $\Delta\Pi=15$ atm; (□) $d=100$, $\Delta\Pi=17$ atm. The solid lines correspond to the best numerical adjustment of the data with Eq. (2). (b) Evolution of $dX/dt(t=0)$ in logarithmic scale with $1-1/d$. The solid line corresponds to an exponential adjustment.

decreases under tensile stress in a complex manner, which nonetheless must be linear in applied stress and ionic volume, λ^3. The activation energy is expected to be linearly modified by the tensile stress as $E(\tau)=E_a-\tau\lambda^3$.

The osmotic pressure difference $\Delta\Pi$ can be approximated as $\Delta\Pi=RT(2C_i-2C_e-C_{\text{sugar}})\sim RT(2C_i-C_{\text{sugar}})$ since C_e can be neglected as long as the globule volume fraction remains small, C_{sugar} is the final sugar concentration imposed by the dilution, and R is the ideal gas constant. $\Delta\Pi$ can now be expressed as $\Delta\Pi=2RTC_{i0}(1-X-1/d)$, where C_{i0} is the initial internal salt concentration and d is the dilution factor of the external phase that sets the initial osmotic pressure difference $\Delta\Pi_0$. Thus, Eq. (1) becomes $dX/dt=\beta(X)(1-X)$ and the characteristic relaxation rate $\beta(X)$ can be expressed as

$$\beta(X)=\beta_0\exp[\varepsilon(1-1/d)]\exp(-\varepsilon X), \tag{2}$$

with $\varepsilon=(a/\delta)(\lambda^3/k_BT)(RTC_{i0})$. In kT units, $\varepsilon(1-1/d)$ is the initial drop of the activation energy induced by the initial tensile stress. Thus, at short time when few ions have diffused through the shells and the osmotic shock is still at its maximum, the permeation rate β increases by the large factor $\exp[\varepsilon(1-1/d)]$. At longer time the second term $\exp(-\varepsilon X)$, which reflects the equilibration of the osmotic stress, slows down the relaxation rate. A plot of $\log[dX/dt(t=0)]$, as a function of $1-1/d$ is linear with slope ε, as seen in Fig. 3(b). From the slope we find $\varepsilon=2.5\pm0.3$.

Equation (2) can be numerically solved and compared to our data as shown in Fig. 3(a). In this fit we also take into account the nonideal dependence of the osmotic pressure with the sugar and salt concentrations [15]. The fit is remarkable and allows for the determination of the two unknown parameters ε and β_0. The time evolution reflects the exponential decrease in diffusion as the osmotic pressure tends toward equilibration causing the stress to decrease and activation energy to increase. It provides another measure of the enhancement of the permeation rate by stress to be compared with the values obtained by varying the initial osmotic shock, Fig. 3(b) ($\varepsilon=4.1\pm1.4$ and $\beta_0=8\pm6\ 10^{-4}$ min^{-1}). With $\delta=100$ nm we get $\lambda=0.6$ nm comparable to the size of a hydrated ion, as expected from the Eyring picture.

The present work offers the first direct experimental evidence that an imposed tensile stress linearly reduces the local energy barrier for an activated process, leading to an exponential increase in diffusion and permeability as envisioned by Eyring almost 100 years ago. The colloidal scale of our system ensures a large surface to volume ratio and smaller forces for a given stress or pressure. Macroscopic systems might fail at these stresses, but the colloidal scale allows for this convincing and straightforward verification of Eyring's ideas.

Practically our findings should provide some guidance in colloidal controlled drug delivery systems and encapsulation design.

We thank E. Bertrand and F. Leal-Calderon for fruitful discussions.

[1] B. F. Gibbs, S. Kermasha, I. Alli, and C. N. Mulligan, Int. J. Food Sci. Nutr. **50**, 213 (1999).
[2] E. L. Chaikof, Annu. Rev. Biomed. Eng. **1**, 103 (1999).
[3] S. Magdassi, Colloids Surf., A **123-124**, 671 (1997).
[4] B. J. Zwolinski, H. Eyring, and C. E. Reese, J. Phys. Colloid Chem. **53**, 1426 (1949).
[5] H. Eyring, J. Chem. Phys. **4**, 283 (1936).
[6] J. Guery, E. Bertrand, C. Rouzeau, P. Levitz, D. A. Weitz, and J. Bibette, Phys. Rev. Lett. **96**, 198301 (2006).
[7] The crystallizable oil DM is a mixture of saturated fatty acids from C8 to C18 (Suppocire DM from Gattefossé).
[8] C. Goubault, K. Pays, D. Olea, P. Gorria, J. Bibette, V. Schmitt, and F. Leal-Calderon, Langmuir **17**, 5184 (2001).
[9] C. Mabille, V. Schmitt, P. Gorria, F. Leal-Calderon, V. Faye, B. Deminière, and J. Bibette, Langmuir **16**, 422 (2000).
[10] The size distribution of the emulsions is measured by static

light scattering (Malvern Mastersizer granulometer).

[11] The surfactant used to stabilize the W/O emulsion is a PEG-30 dipolhydroxystearate (Arlacel P135 from Uniquema) and the one used for the O/W emulsion is a mixture of monoglycerides, diglycerides, and triglycerides and of monomesters, dimesters, and trimesters of PEG and fatty acids (Gelucire 4414 from Gattefossé).

[12] The potentiometric device is composed of an Ag/AgCl specific electrode (Radiometer, France), a K_2SO_4 reference electrode (Radiometer, France) and a data acquisition board (AT_MIO 16E–10, National Instruments).

[13] K. Pays, J. Giermanska-Kahn, B. Pouligny, J. Bibette, and F. Leal-Calderon, J. Controlled Release **79**, 193 (2002).

[14] K. B. McAfee, J. Chem. Phys. **28**, 218 (1958).

[15] *Handbook of Chemistry and Physics*, edited by R. C. Weast (CRC, Boca Raton, FL, 1978).